arXiv:1703.10024v2 [cond-mat.mes-hall] 25 Apr 2017

Squeezed thermal reservoirs as a resource for a nano-mechanical engine beyond the Carnot limit

Jan Klaers[1]* and Stefan Faelt[1], Atac Imamoglu[1], and Emre Togan[1]
[1] *Institute for Quantum Electronics, ETH Zürich, CH-8093 Zürich, Switzerland*

The efficient conversion of thermal energy to mechanical work by a heat engine is an ongoing technological challenge. Since the pioneering work of Carnot, it is known that the efficiency of heat engines is bounded by a fundamental upper limit - the Carnot limit. Theoretical studies suggest that heat engines may be operated beyond the Carnot limit by exploiting stationary, non-equilibrium reservoirs that are characterized by a temperature as well as further parameters. In a proof-of-principle experiment, we demonstrate that the efficiency of a nano-beam heat engine coupled to squeezed thermal noise is not bounded by the standard Carnot limit. Remarkably, we also show that it is possible to design a cyclic process that allows for extraction of mechanical work from a single squeezed thermal reservoir. Our results demonstrate a qualitatively new regime of non-equilibrium thermodynamics at small scales and provide a new perspective on the design of efficient, highly miniaturized engines.

I. INTRODUCTION

Advances in micro- and nano-technology allow for testing concepts derived from classical thermodynamics in regimes where the underlying assumptions, such as the thermodynamic limit and thermal equilibrium, no longer hold [1–6]. Extremely miniaturized forms of heat engines, where the working medium is represented by a single particle, have revealed a fluctuation-dominated regime in the conversion of heat to work far away from the thermodynamic limit [7–11]. By employing non-equilibrium reservoirs it is furthermore expected that the efficiency of work generation surpasses the standard Carnot limit [12], as has been theoretically suggested for quantum coherent [13], quantum correlated [14, 15] and squeezed thermal reservoirs [16–20].

In optics, the electric field of a monochromatic wave can be decomposed into two quadrature components that vary as $\cos\omega t$ and $\sin\omega t$ respectively. For coherent states such as laser light, the uncertainties in the two quadratures are equal and follow the lower bound of Heisenberg's uncertainty relation. By contrast, squeezed states of light have reduced fluctuations in one (squeezed) quadrature at the cost of enhanced fluctuations in the other (anti-squeezed) quadrature allowing for optical measurements with reduced quantum noise [21, 22]. Squeezed states are, however, neither restricted to electromagnetic waves nor to minimum uncertainty states. For example, a mechanical oscillator may be prepared in a squeezed thermal state [23–25] by a periodic modulation of the spring constant [26]. This results in a state with reduced thermal fluctuations in one quadrature (e.g. momentum) and enhanced thermal fluctuations in the other quadrature (e.g. position) compared to the expected level of fluctuations at the given temperature. In the context of heat engines, a theoretical work by Roßnagel et al. [17] suggests that squeezed thermal states may be used as an additional resource to overcome the standard Carnot limit. Due to the non-equilibrium nature of squeezed thermal reservoirs, this result does not violate the second law of thermodynamics. In our work, we present a physical realization of such an engine with a working medium consisting of a vibrating nano-beam that is driven by squeezed electronic noise to perform work beyond the standard Carnot limit. Furthermore, we demonstrate that by a phase-selective coupling to the squeezed or anti-squeezed quadrature, work can be extracted even from a single squeezed reservoir, which is not possible with a standard thermal reservoir [13, 27].

II. NANO-BEAM HEAT ENGINE

Figure 1a shows a sketch of the experiments: The working medium of our heat engine consists of a single harmonic oscillator given by the fundamental flexural mode of a doubly-clamped (GaAs) nano-beam structure with eigenfrequency $\nu = \omega/2\pi = 1.97\,\mathrm{MHz}$, quality factor of order $Q \simeq 10^3$ at room temperature and under vacuum conditions ($p \simeq 10^{-4}\,\mathrm{mbar}$). The beam has a length of $18.8\,\mu\mathrm{m}$, width of $2\,\mu\mathrm{m}$, thickness of 270 nm, and is fabricated using conventional nano-structuring techniques such as electron beam lithography and selective etching. In the growth direction the beam contains two doped layers, which allow us to apply electric fields across the beam material. These electric fields lead to forces being applied to the beam structure due to the piezo-electricity of the employed gallium arsenide material. When driven by a noisy waveform, this creates a random force that allows us to mimic an engineered thermal environment for the beam structure. The waveform is synthesized from two independent white noise signals $\xi_{1,2}(t)$ that are mixed with sine and cosine component of a phase reference at frequency ν leading to a stochastic force $f(t) = a_0\left[\mathrm{e}^{+\tilde{r}}\xi_1(t)\cos(\omega t) + \mathrm{e}^{-\tilde{r}}\xi_2(t)\sin(\omega t)\right]$. A positive squeezing parameter $\tilde{r}$ corresponds to an amplified cosine and attenuated sine component at frequency ν in the thermal bath, while the overall strength of the noise can be controlled by the amplitude a_0.

* jklaers@phys.ethz.ch

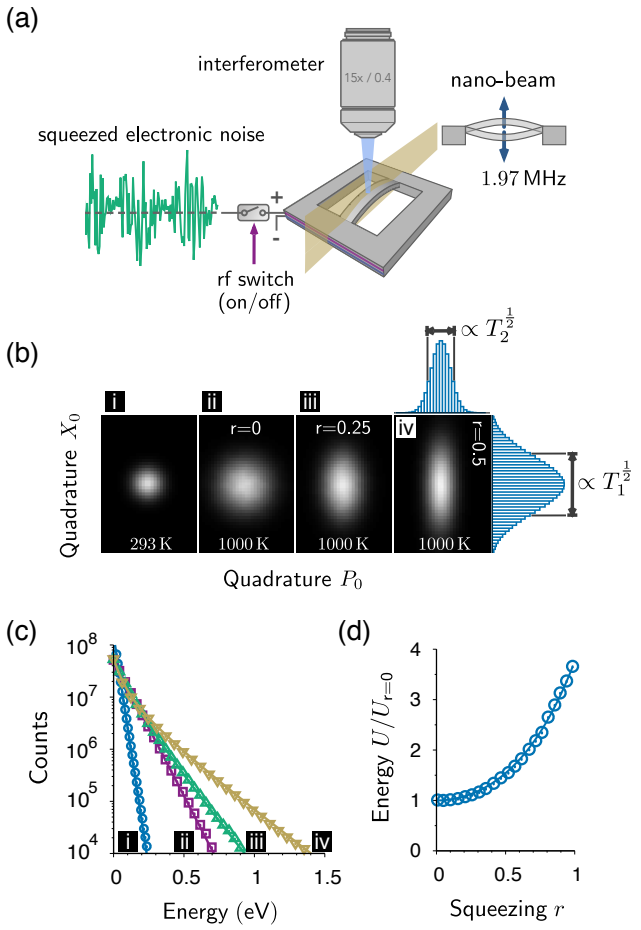

Figure 1. Nano-beam heat engine. (a) Doubly-clamped nano-beam piezo-electrically coupled to squeezed electronic noise. (b) Phase space density of the nano-beam motion (in rotating frame), (i) when no additional noise is applied, (ii)-(iv) when (squeezed) noise is applied. The fluctuations in position and momentum are characterized by two temperature parameters $T_{1,2}$ proportional to the Gaussian variance of the line integrated probability densities. The temperature is $T = 293\,\mathrm{K}$ for (i), and $T = \sqrt{T_1 T_2} \simeq 1000\,\mathrm{K}$ for (ii-iv). The squeezing parameter follows $r = 0$ for (i-ii), and $r = \ln(T_1/T_2)/4 = 0.25,\ 0.5$ for (iii-iv). (c) Measured energy histogram (symbols) of the nano-beam motion in a (squeezed) thermal state. The solid lines show the theoretically expected distributions. Experimental parameters as in Fig. 1b. (d) Average energy of the nano-beam motion (circles) as a function of the squeezing parameter r. The energies are normalized to the energy at vanishing squeezing $U_{r=0} = k_\mathrm{B}T$, with the temperature of the system being kept fixed. The solid line corresponds to the theoretical expectation $U/U_{r=0} = 1 + 2\sinh^2 r$. Statistical errors (s.e.m.) are smaller than the symbol size for all data points.

To demonstrate the generation of squeezed thermal states, we experimentally determine the motional state of the nano-beam by recording the instantaneous position (out-of-plane displacement) of the beam via Mach-Zehnder interferometry [28] and calculating the corresponding phase-space probability distribution, see Fig. 1b. In the absence of additional noise ($a_0 = 0$), the nano-beam motion is fully determined by the residual thermal noise at room temperature, see panel (i) in Fig. 1b. By increasing the noise amplitude a_0, the state of the nano-beam can be prepared in a thermal state at higher temperature $T = 1000\,\mathrm{K}$, see panel (ii). Squeezed noise leads to the expected elliptical phase-space probability distribution, see panels (iii) and (iv). We emphasize that all results are presented in a position-momentum-frame that rotates with frequency ν with respect to the laboratory frame. The observed probability densities closely follow the theoretically expected Gaussian distribution [23]

$$\rho(x_0, p_0) \propto \exp\left(-\frac{\hbar\omega x_0^2}{2k_\mathrm{B}T_1} - \frac{\hbar\omega p_0^2}{2k_\mathrm{B}T_2}\right), \qquad (1)$$

where x_0, p_0 are dimensionless position and momentum variables and T_1, T_2 are two temperature parameters describing the level of fluctuations in the anti-squeezed and squeezed quadratures (proportional to the variance of the gaussian distribution). These parameters are related to the effective temperature and squeezing parameter of the system by $T_{1,2} = T\exp(\pm 2r)$ [23, 25]. The corresponding energy histograms reveal exponential distributions for cases (i) (circles) and (ii) (boxes) as is expected from purely thermal states (Fig. 1c). The non-exponential decays for parameter sets (iii) (upright triangles) and (iv) (upside-down triangles) demonstrate the non-equilibrium nature of the state of the nano-beam. The solid lines in Fig. 1c show the theoretically expected energy distribution $\rho(E) \propto I_0\left(E\sinh(2r)/k_\mathrm{B}T\right)\exp\left(-E\cosh(2r)/k_\mathrm{B}T\right)$ with I_0 as the modified Bessel function of order zero [28]. Finally, the mean energy U of the nano-beam motion as a function of the squeezing parameter r (at fixed temperature) closely follows the caloric equation of state $U = k_\mathrm{B}T\left(1 + 2\sinh^2 r\right)$, as demonstrated in Fig. 1d.

In our experiment, the eigenfrequency of the fundamental flexural mode can be tuned over a few 100 kHz by applying a DC electrical potential to the nano-beam [28] allowing for a cyclic process with work output. The extraction of work in an engine is normally realized by an increase in volume of a gaseous working medium driving a piston. For a harmonically trapped working medium, such as the one investigated here, an expansion of the working medium may be realized by a decrease in trapping frequency ω. The latter suggests to define the volume of the system as the inverse trapping frequency $V = \omega^{-1}$, see Ref. [29]. With this, a relation similar to the state functional formulation of the first law of thermodynamics holds [28]

$$dU = T_1 dS_1 + T_2 dS_2 - p dV\,, \qquad (2)$$

with $S_1 = -k_\mathrm{B}\int_{-\infty}^{+\infty}\rho(x_0)\ln(\rho(x_0))\,dx_0$ as the entropy of the anti-squeezed quadrature and the corresponding definition for S_2 being obtained by replacing x_0 with p_0. The

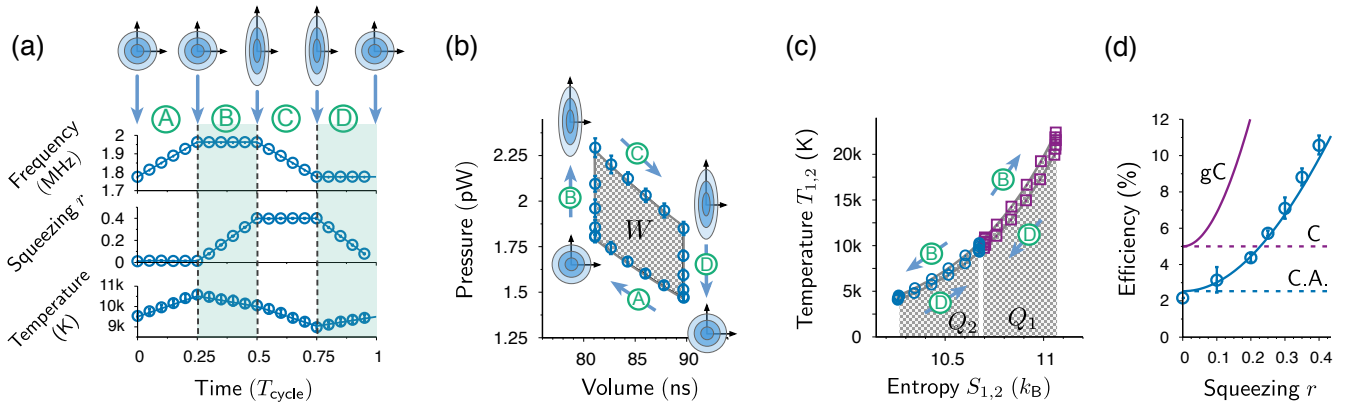

Figure 2. Otto cycle between a cold thermal and a hot squeezed thermal reservoir. (a) Frequency, squeezing and temperature of the nano-beam motion throughout one cycle of the engine ($T_{\rm cycle}$ amounts to several seconds). The shown protocol implements an Otto cycle at maximum power between a cold thermal reservoir at $T_{\rm c} = 9,500\,{\rm K}$ and a hot squeezed reservoir at $T_{\rm h} = 10,000\,{\rm K}$ with squeezing parameter $r = 0.4$. The four consecutive strokes include an isentropic compression (A), isochoric heat addition (B), isentropic expansion (C) and isochoric heat rejection (D). (b) Pressure-volume diagram of the Otto cycle. The shaded area corresponds to the total work output W performed by the engine. The solid line represents the theoretically expected behavior. (c) Temperature-entropy diagram of the Otto cycle. T_1 (T_2) and S_1 (S_2) denote temperature and entropy of the anti-squeezed (squeezed) quadrature. The solid line shows the theoretical expectations. (d) Efficiency of the nano-beam heat engine as a function of the squeezing parameter of the hot reservoir (circles). The solid blue line shows the theoretical expectation $\eta = 1 - \sqrt{T_{\rm c}/T_{\rm h}}\,/\cosh(r)$. The measured engine efficiency surpasses the standard Carnot (C) and Curzon-Ahlborn (C.A.) efficiency for finite squeezing parameters (dashed horizontal lines), but obeys a generalized Carnot limit (gC) [17, 27]. All error bars indicate statistical errors (s.e.m.) except for Fig. 2d (see Ref. [28] for details).

pressure is defined by $p = -(\partial U/\partial V)_{S_1,S_2}$, which evaluates to $p = U/V$ for the given system. In this way, the term $-p\,dV$ represents the work associated to a change in volume or trapping frequency, whereas the terms $T_i\,dS_i$ with $i = 1, 2$ describe heat exchange with the environment.

III. OTTO CYCLE WITH SQUEEZED THERMAL RESERVOIRS

In a first line of experiments, we construct an Otto cycle between a hot squeezed thermal reservoir at $T_{\rm h} = 10,000\,{\rm K}$ with squeezing factor $r = 0.4$ and a cold purely thermal bath at $T_{\rm c} = 9,500\,{\rm K}$ under maximum power condition [17]. The four strokes include an adiabatic compression, isochoric heat addition, adiabatic expansion and isochoric heat rejection. Similar to colloidal heat engines [9], the working medium in our system cannot be fully decoupled from its environment rendering the implementation of adiabatic steps not obvious. Experimentally, it is however feasible to replace the adiabatic steps by isentropic steps. The isentropic steps are implemented by simultaneously varying frequency and temperature such that the ratios $T_{1,2}/\omega$ remain constant, which conserves the entropies $S_{1,2}$ [28]. Figure 2a shows frequency, squeezing and temperature of the nano-beam state throughout one cycle of the engine under quasi-static operation (the cycle time $T_{\rm cycle}$ amounts to several seconds). The pressure-volume (p-V) and temperature-entropy (T-S) diagrams are shown in Fig. 2b,c. The shaded area in the p-V diagram corresponds to a net work output of $W \simeq 26\,{\rm meV}$ performed per cycle. We point out that presently, this work is neither used to perform a certain task, nor stored in some form of potential energy. The T-S diagram is composed of two closed curves corresponding to temperature and entropy variation of the squeezed (circles) and anti-squeezed quadrature (boxes) within one cycle. Note that the curve for the anti-squeezed quadrature is run through clockwise, while the curve for the squeezed quadrature is run through counterclockwise. The net amount of heat consumed from the environment $Q_{\rm h}$ during the hot isochore (B) corresponds to the difference of the two shaded areas, which is $Q_{\rm h} = Q_1 - Q_2 \simeq 244\,{\rm meV}$. The efficiency of the cycle finally evaluates to $\eta = W/Q_{\rm h} = (10.6 \pm 0.5)\%$, which is roughly twice the efficiency of a Carnot cycle operating between $T_{\rm h}$ and $T_{\rm c}$ and four times the Curzon-Ahlborn efficiency [30]. We emphasize that the costs of providing a squeezed thermal bath are not accounted for in our analysis, which is fully analogous to neglecting the costs of providing a hot or cold bath in standard thermodynamics. Figure 2d shows the efficiency for varying squeezing parameters of the hot bath. The solid blue line corresponds to the theoretical expectation $\eta = 1 - \sqrt{T_{\rm c}/T_{\rm h}}\,/\cosh(r)$, see Ref. [17, 28], whereas the two horizontal dashed lines show the (standard) Carnot (C) and Curzon-Ahlborn (C.A.) efficiencies given by $\eta_{\rm Carnot} = 1 - T_{\rm c}/T_{\rm h}$ and $\eta_{\rm C.A.} = 1 - \sqrt{T_{\rm c}/T_{\rm h}}$ respectively. These results clearly demonstrate that squeezing, given as a free resource, can be used to increase the work output and efficiency of an

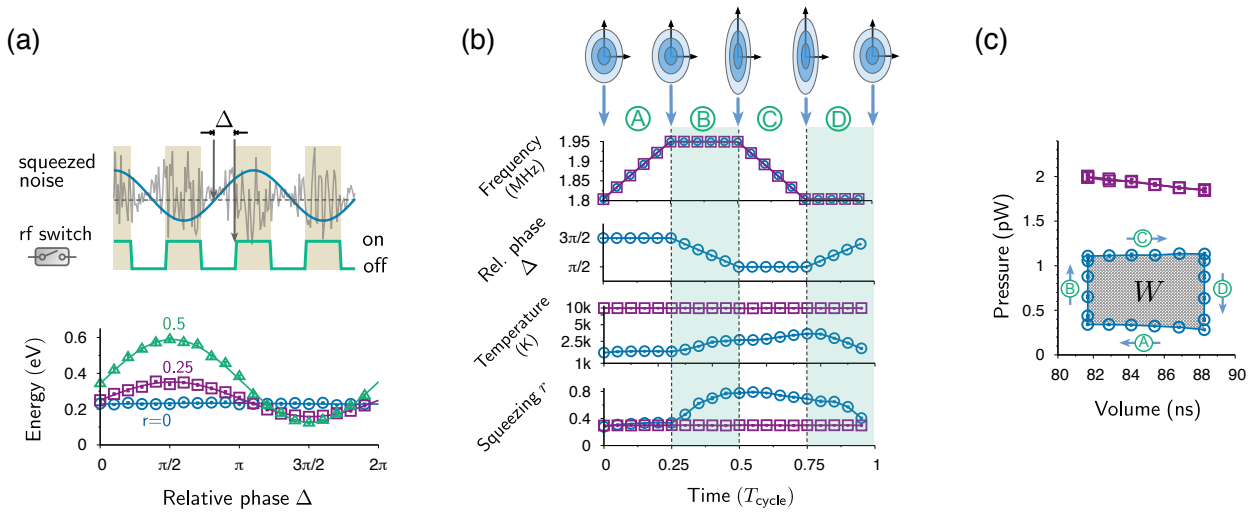

Figure 3. Work extraction from a single squeezed thermal reservoir. (a) By means of a radio-frequency switch (rf switch in Fig. 1a) the coupling between the squeezed electronic noise and the nano-beam is periodically switched on and off with the phase difference between the phase of the squeezed noise and the switching being denoted by Δ (top). Mean energy of the working medium coupled to a squeezed bath as a function of the relative phase Δ for three squeezing parameters $r = 0, 0.25, 0.5$ (bottom). The data points are interpolated by harmonic functions with varying amplitude and offset (solid lines). (b) Protocol to extract work from a single squeezed reservoir with $T = 10,000\,\mathrm{K}$ and $r = 0.3$ by periodically varying mechanical eigenfrequency ν and phase Δ (circles in upper two graphs). The four strokes include an isophasal compression, during which the phase relation between squeezed noise and periodic coupling is kept fixed, an isochoric heat addition, isophasal expansion, and isochoric heat rejection. Temperature and squeezing of the nano-beam motional state as consequence of the applied protocol (circles in lower two graphs). The case of an unmodulated coupling is shown with box symbols. Lines between data points are guides to the eye. (c) Pressure-volume diagram revealing a finite amount of work ($W \simeq 37\,\mathrm{meV}$) extracted from the single squeezed reservoir per cycle (circles). No work output is observed for unmodulated coupling (boxes). Lines between data points are guides to the eye. Statistical errors (s.e.m.) are smaller than the symbol size for all data points.

engine beyond the (standard) Carnot limit. The engine operation, however, does obey a generalized Carnot limit (solid line 'gC') [17, 27].

IV. WORK EXTRACTION FROM A SINGLE RESERVOIR

In a second line of experiments, we eliminate the cold thermal heat bath in the operation of the engine and introduce a phase-selective thermal coupling that will allow to periodically extract work from a single squeezed heat bath. In these measurements, the coupling of the mechanical oscillator to the squeezed electronic noise is periodically switched on and off by means of a rectangular control signal with frequency 2ν and duty cycle 50%, see top panel in Fig. 3a, that is applied to a radio-frequency switch. The mean energy of the mechanical oscillator as a function of the relative phase Δ between the phase of the switching function and the phase of the squeezed bath is shown in the bottom panel of Fig. 3a for three different squeezing parameters. For non-vanishing squeezing parameters (boxes and triangles), the measured energy reaches a maximum when the oscillator is coupled to the anti-squeezed quadrature of the bath at $\Delta_{\max} \simeq \pi/2$, whereas an energy minimum is obtained for coupling to the squeezed quadrature at $\Delta_{\min} \simeq 3\pi/2$. This phase-selective coupling allows us to extract work from a single squeezed reservoir by a periodic variation of mechanical frequency and phase difference Δ as shown in the upper two panels of Fig. 3b (circles). The four strokes include an "isophasal" compression, during which the phase relation between squeezed noise and periodic coupling is kept fixed, an isochoric heat addition, isophasal expansion, and isochoric heat rejection. Temperature and squeezing of the nano-beam state as consequence of the applied protocol are shown in the bottom two panels of Fig. 3b (circles). Finally, the p-V diagram in Fig. 3c clearly reveals a finite amount of work ($W \simeq 37\,\mathrm{meV}$) that is extracted from the single squeezed reservoir per cycle (circles). Compared to the case of an unmodulated coupling (switch in 'on' position), resulting in a squeezed thermal state with $T = 10,000\,\mathrm{K}$ and $r = 0.3$ throughout the cycle (boxes in Fig. 3b, c), the working medium operates at a reduced temperature. The latter originates from the incomplete decoupling of the oscillator from its environment during the 'off'-phases of the phase-selective coupling. Here, an improved isolation would further increase the extracted work per cycle.

V. CONCLUSIONS

Single-particle heat machines provide an excellent platform to test theoretical advances in and our understanding of thermodynamics at the micro- and nano-scale. In

this work, a minimalist heat engine has been realized that takes advantage of squeezed heat to outperform conventional heat engines. The non-equilibrium nature of these reservoirs permit work extraction from a single reservoir and engine efficiencies unbounded by the standard Carnot limit. A major open question remains whether highly miniaturized heat engines, such as the one reported here, will be able to use the extracted work to accomplish mesoscopic tasks as transporting particles [31] or manipulating biological matter [32]. Squeezed thermal noise may naturally arise in non-equilibrium environments with temporally or spatially modulated temperature profiles and could be used to fuel such devices.

[1] J. Liphardt, S. Dumont, S. B. Smith, I. Tinoco, and C. Bustamante, *Equilibrium information from nonequilibrium measurements in an experimental test of Jarzynski's equality*, Science **296**, 1832 (2002).

[2] S. Toyabe, T. Sagawa, M. Ueda, E. Muneyuki, and M. Sano, *Experimental demonstration of information-to-energy conversion and validation of the generalized Jarzynski equality*, Nature Phys. **6**, 988 (2010).

[3] A. Bérut, A. Arakelyan, A. Petrosyan, S. Ciliberto, R. Dillenschneider, and E. Lutz, *Experimental verification of Landauer's principle linking information and thermodynamics*, Nature **483**, 187 (2012).

[4] S. Trotzky, Y. A. Chen, A. Flesch, I. P. McCulloch, U. Schollwöck, J. Eisert, and I. Bloch, *Probing the relaxation towards equilibrium in an isolated strongly correlated one-dimensional Bose gas*, Nature Phys. **8**, 325 (2012).

[5] É. Roldán, I. A. Martínez, J. M. R. Parrondo, and D. Petrov, *Universal features in the energetics of symmetry breaking*, Nature Phys. **10**, 457 (2014).

[6] For a recent review see: S. Vinjanampathy, and J. Anders, *Quantum thermodynamics*, Contemp. Phys. **57**, 1 (2016), arXiv preprint arXiv:1508.06099.

[7] V. Blickle, and C. Bechinger, *Realization of a micrometre-sized stochastic heat engine*, Nature Phys. **8**, 143 (2012).

[8] J. V. Koski, V. F. Maisi, J. P. Pekola, and D. V. Averin, *Experimental realization of a Szilard engine with a single electron*, P. Natl. Acad. Sci. USA **111**, 13786 (2014).

[9] I.A. Martínez, É. Roldán, L. Dinis, D. Petrov, J. M. Parrondo, and R. A. Rica, *Brownian Carnot engine*, Nature Phys. **12**, 67 (2016).

[10] J. Roßnagel, S. T. Dawkins, K. N. Tolazzi, O. Abah, E. Lutz, F. Schmidt-Kaler, and K. A. Singer, *A single-atom heat engine*, Science **352**, 325 (2016).

[11] S. Krishnamurthy, S. Ghosh, D. Chatterji, R. Ganapathy, and A. K. Sood, *A micrometre-sized heat engine operating between bacterial reservoirs*, Nature Phys. **12**, 1134 (2016).

[12] S. Carnot, *Réflexions sur la puissance motrice du feu et sur les machines propres a développer cette puissance*, Bachelier, Paris (1824).

[13] M. O. Scully, M. S. Zubairy, G. S. Agarwal, and H. Walther, *Extracting work from a single heat bath via vanishing quantum coherence*, Science **299**, 862 (2003).

[14] R. Dillenschneider and E. Lutz, *Energetics of quantum correlations*, EPL **88**, 50003 (2009).

[15] M. Perarnau-Llobet, K. V. Hovhannisyan, M. Huber, P. Skrzypczyk, N. Brunner, and A. Acín, *Extractable work from correlations*, Phys. Rev. X **5**, 041011 (2015).

[16] X. L. Huang, T. Wang, and X. X. Yi, *Effects of reservoir squeezing on quantum systems and work extraction*, Phys. Rev. E **86**, 051105 (2012).

[17] J. Roßnagel, O. Abah, F. Schmidt-Kaler, K. Singer, and E. Lutz, *Nanoscale heat engine beyond the Carnot limit*, PRL **112**, 030602 (2014).

[18] L. A. Correa, J. P. Palao, D. Alonso, and G. Adesso, *Quantum-enhanced absorption refrigerators*, Sci. Rep. **4**, 3949 (2014).

[19] W. Niedenzu, D. Gelbwaser-Klimovsky, A. G. Kofman, and G. Kurizki, *On the operation of machines powered by quantum non-thermal baths*, New J. Phys. **18**, 083012 (2016).

[20] W. Niedenzu, V. Mukherjee, A. Ghosh, A. G. Kofman, and G. Kurizki, *Universal thermodynamic limit of quantum engine efficiency*, arXiv:1703.02911 (2017).

[21] LIGO Scientific Collaboration, *A gravitational wave observatory operating beyond the quantum shot-noise limit*, Nature Phys. **7**, 962 (2011).

[22] F. Wolfgramm, A. Cere, F. A. Beduini, A. Predojević, M. Koschorreck, and M. W. Mitchell, *Squeezed-light optical magnetometry*, PRL **105**, 053601 (2010).

[23] H. Fearn and M. J. Collett, *Representations of squeezed states with thermal noise*, J. Mod. Optic. **35**, 553 (1988).

[24] M. S. Kim, F. A. M. de Oliveira, and P. L. Knight, *Properties of squeezed number states and squeezed thermal states*, Phys. Rev. A **40**, 2494 (1989).

[25] R. R. Tucci, *Entropy of a harmonic oscillator in contact with a squeezed reservoir*, Int. J. Mod. Phys. B **5**, 545 (1991).

[26] D. Rugar and P. Grütter, *Mechanical parametric amplification and thermomechanical noise squeezing*, PRL **67**, 699 (1991).

[27] O. Abah and E. Lutz, *Efficiency of heat engines coupled to non-equilibrium reservoirs*, EPL **106**, 20001 (2015).

[28] See supplemental material for further experimental and theoretical details.

[29] V. Romero-Rochín, *Equation of state of an interacting Bose gas confined by a harmonic trap: The role of the "harmonic" pressure*, PRL **94**, 130601 (2005).

[30] F. L. Curzon and B. Ahlborn, *Efficiency of a Carnot engine at maximum power output*, Am. J. Phys. **43**, 22 (1975).

[31] P. Hänggi and F. Marchesoni, *Artificial Brownian motors: Controlling transport on the nanoscale*, Rev. Mod. Phys. **81**, 387 (2009).

[32] S. M. Douglas, I. Bachelet, and G. M. Church, *A logic-gated nanorobot for targeted transport of molecular payloads*, Science **335**, 831 (2012).